

The EUMETSAT
Network of
Satellite Application
Facilities



Document NWPSAF-MO-TR-032

Version 1.0

24/05/16

NWP SAF AMV monitoring: the 7th Analysis Report (AR7)

Francis Warrick

Met Office, UK



NWP SAF AMV monitoring: the 7th Analysis Report (AR7)

Francis Warrick

Met Office, UK

This documentation was developed within the context of the EUMETSAT Satellite Application Facility on Numerical Weather Prediction (NWP SAF), under the Cooperation Agreement date 29 June 2011, between EUMETSAT and the Met Office, UK, by one or more partners within the NWP SAF. The partners in the NWP SAF are the Met Office, ECMWF, KNMI and Météo France.

Copyright 2016, EUMETSAT, All Rights Reserved.

Change Record			
Version	Date	Author / changed by	Remarks
0.1	30/4/16	F Warrick	First draft.
0.2	17/5/16	F Warrick	Updates following comments from Mary Forsythe
1.0	24/5/16	F Warrick	Version for publication following comments from Mary Forsythe and Roger Saunders.

Contents

1	Introduction	4
2	Index of Features	7
3	Low Level Updates	8
	Feature 2.7 Spuriously Fast Meteosat and MTSAT Winds	8
4	Mid Level Updates	11
	Features 2.8 and 2.9: Positive Bias in the Tropics, Negative Bias in the Extra-Tropics . . .	11
5	High Level Updates	14
	Feature 2.13. Tropics Positive Speed Bias	14
	Feature 5.3. MTSAT Tropical Cyclone Speed Bias	17
	Feature 6.3. Very High FY-2E WV Winds	18
6	Polar Wind Updates	21
	Feature 7.1. Dual-Metop Positive Bias in Tropics	21
	Feature 7.2. EUMETSAT Metop High Level Negative Bias in Extra-Tropics	22
	Feature 7.3 MISR Fast Bias over Ice and Desert	22
	Feature 7.4 LeoGeo Coverage Gaps at Particular Longitudes	29
	Feature 7.5 Stripes of Large O-Bs in MISR data.	30
	Feature 7.6. Square-Shaped Spatial Distribution of Suomi-NPP Winds.	33
7	Summary	34
	References & Acknowledgements	35

1 Introduction

The aim of the NWP SAF (Satellite Application Facility for Numerical Weather Prediction) atmospheric motion vector (AMV) monitoring, nwpsaf.eu/site/monitoring/winds-quality-evaluation/amv/, is to identify and understand AMV errors so that both their derivation and their usage in NWP can be improved. As part of the NWP SAF AMV monitoring, an archive of observation-minus-background (O-B) monitoring statistics is maintained. O-Bs are the difference between AMVs and co-located short-range NWP model winds. The O-Bs are measured against Met Office and ECMWF global model backgrounds, to help reveal whether features seen in the O-Bs are due to problems with one or both models, or with the AMVs.

To make sense of the large amount of monitoring information held on the website, every two years an Analysis Report is produced. These assess whether features seen in the monitoring statistics have improved or worsened, and identify any new features which have appeared since the previous report. In some cases the cause of a feature can be investigated using a mix of additional O-B statistics, height assignment differences (between the AMVs, model best-fit pressures and cloud-top height products), model fields and satellite imagery. This document marks the seventh in the series of analysis reports (AR7). Previous analysis reports are hereafter referred to as AR6 (2014), AR5 (2012), AR4 (2010), AR3 (2008), AR2 (2005) and AR1 (2001) and are available to download from the website.

The datasets included in the AMV monitoring as of March 2016 are listed in Table 1. A list of datasets added or removed since AR6 is shown in Table 2. Significant changes seen in the monitoring since AR6 include:

1. **Himawari-8 AMVs.** AMVs from the next-generation JMA geostationary satellite Himawari-8 became available in July 2015. This satellite replaces MTSAT-2, from which AMV generation ended in March 2016. Differences with MTSAT-2 include: higher resolution imagery, a new tracking scheme, a new height assignment scheme and 2 new water vapour channels. The new tracking combines information from tracking with both a large and a small target box [1]. The height assignment minimises differences between model radiance and observed cloud radiance, and between model wind and observed wind. Large changes are seen in the O-Bs, volume of data and vertical coverage.

2. **EUMETSAT Metop AMVs** The coverage of the EUMETSAT Single-Metop AMV product has gradually been extended since AR6. Initially winds were available as far equatorwards as 50° N/S, but now the full overlap area available by tracking with image pairs is used, with some EUMETSAT Single-Metop AMVs available as far equatorwards as 40° N/S. Dual-Metop AMVs have been added

to the NWP SAF monitoring which are the first AMV dataset to provide global AMV coverage. Using images from a single polar orbiter, AMVs can only be derived in the polar regions where consecutive image swaths overlap. However, as the two Metop satellites' orbits are only around 50 minutes apart, consecutive swaths of Metop imagery are partially overlapping at all latitudes, allowing for global AMV derivation from polar imagery using one image from each Metop. Changes to the EUMETSAT Metop derivation scheme led to significant changes in Metop AMV O-B characteristics since AR6.

Geostationary AMVs	Channels
Meteosat-10	IR 10.8, WV 6.2, WV 7.3, VIS 0.8, HRVIS
Meteosat-9	IR 10.8, WV 6.2, WV 7.3, VIS 0.8, HRVIS
Meteosat-7	IR, WV, VIS
GOES-13 (+unedited)	IR 10.7, IR 3.8, WV, VIS
GOES-15 (+unedited)	IR 10.7, IR 3.8, WV, VIS
Himawari-8	IR, WV 6.2, WV 6.7, WV 7.3, VIS
INSAT-3D	IR, IR 3.8, WV, VIS
Kalpana	IR, WV
FY-2E	IR, WV
FY-2G	IR, WV
COMS-1	IR, IR 3.8, WV, VIS
Polar AMVs	Channels
Aqua MODIS (from NESDIS & DB)	IR, WV, CSWV
Terra MODIS (from NESDIS & DB)	IR, WV, CSWV
Terra MISR (NASA-JPL)	VIS 0.6
NOAA-15 (CIMSS)	IR
NOAA-18/19 (CIMSS & DB)	IR
Metop-A (EUMETSAT, CIMSS)	IR
Metop-B (EUMETSAT, CIMSS)	IR
Suomi-NPP (NESDIS & DB)	IR
Mixed AMVs	Channels
LeoGeo (CIMSS)	IR
Dual-Metop (EUMETSAT)	IR

Table 1: AMV datasets monitored by the NWP SAF. DB = direct broadcast, IR = infrared, VIS = visible, HRVIS = high resolution VIS, WV = cloudy water vapour, CSWV = clear sky WV.

Change	Type	Date	Description
NOAA-16	Removed	6/14	Satellite failure.
Dual-Metop	New	9/14	Added to monitoring.
INSAT-3D	New	1/15	Added to monitoring.
Suomi-NPP	New	2/15	Added to monitoring.
Terra MISR	New	5/15	Added to monitoring.
Himawari-8	Transition	7/15	Replaced MTSAT-2 at 140°E.
MTSAT-2	Removed	3/16	Replaced by Himawari-8.
Terra MODIS (CIMSS)	Removed	4/15	No longer monitored.
Aqua MODIS (CIMSS)	Removed	4/15	No longer monitored.
COMS-1	New	8/15	Added to monitoring.
FY-2G	New	7/15 (EC) 11/15 (MO)	Added to monitoring.

Table 2: Changes to monitoring since AR6.

The report structure is as follows. Section 2 gives an overview of current features identified in the monitoring statistics. Sections 3, 4 and 5 present updates on these features separated by low level (below 700 hPa), mid level (400-700 hPa) and high level (above 400 hPa) respectively. Updates on polar AMV features are described in Section 6. Section 7 is a report summary.

2 Index of Features

Features are referenced in the format X.Y, where X is the number of the analysis report where the feature was first described and Y is the example number from that report. In this report the tropics refer to the area within 20°N/S. Table 3 gives the status of new features and those previously documented, and states for each feature whether an update is given in this report.

Ref.	Feature	AR	Resolved?	Update?
Low Level (below 700 hPa)				
2.3	GOES winter negative bias over NE America	2,3,6	No	N
2.6	MSG positive bias over N Africa	2,3,4,6	No	N
2.7	Spuriously fast Meteosat and MTSAT winds	2,3,4,6	Reduced in Himawari-8	Y
4.1	Model differences in the Pacific	4,5	Differences for GOES	N
5.1	Patagonia negative bias	5	No	N
5.2	MSG negative bias during Somali jet	5,6	No	N
6.1	Bias in tropical E Atlantic	6	No	N
6.2	MTSAT and FY-2E bias during NE winter monsoon	6	Reduced in Himawari-8	N
Mid Level (400-700 hPa)				
2.8	Positive bias in the tropics	2,3,4,5,6	Reduced in Himawari-8	Y
2.9	Negative bias in the extra-tropics	2,3,4,5,6	Reduced in Himawari-8	Y
High Level (above 400 hPa)				
2.10	Jet region negative speed bias	2,3,4,5,6	No	N
2.13	Tropics positive speed bias	2,3,4,5,6	Reduced in Himawari-8	Y
2.14	High troposphere positive bias	2,3,6	No	N
2.15	Differences between channels	2,3,5	Reduced in Himawari-8	N
3.2	Negative Speed bias in TEJ	3,6	No	N
4.2	GOES negative bias in tropical Pacific	4,5,6	No	N
5.3	MTSAT tropical cyclone speed bias	5,6	No	Y
6.3	Very high FY-2E WV winds	6	Yes	Y
Polar AMVs				
2.19	High level positive speed bias	2,3,4,5	No	N
2.20	Low level negative speed bias	2,3,4	No	N
4.3	Near-pole mid level negative bias	4,5	No	N
6.4	EUMETSAT Metop near the poles	6	Errors reduced	N
7.1	Dual-Metop high level positive bias in tropics	New	New	Y
7.2	EUMETSAT Metop high level negative bias in mid-latitudes	New	New	Y
7.3	MISR fast bias over ice and desert	New	New	Y
7.4	LeoGeo coverage gaps at particular longitudes	New	New	Y
7.5	MISR bad orbits	New	New	Y
7.6	VIIRS square distribution	New	New	Y

Table 3: Status of the current features identified in the NWP SAF AMV monitoring. Green shading indicates a new feature, blue indicates a feature that has been fixed or otherwise closed.

3 Low Level Updates

Feature 2.7 Spuriously Fast Meteosat and MTSAT Winds

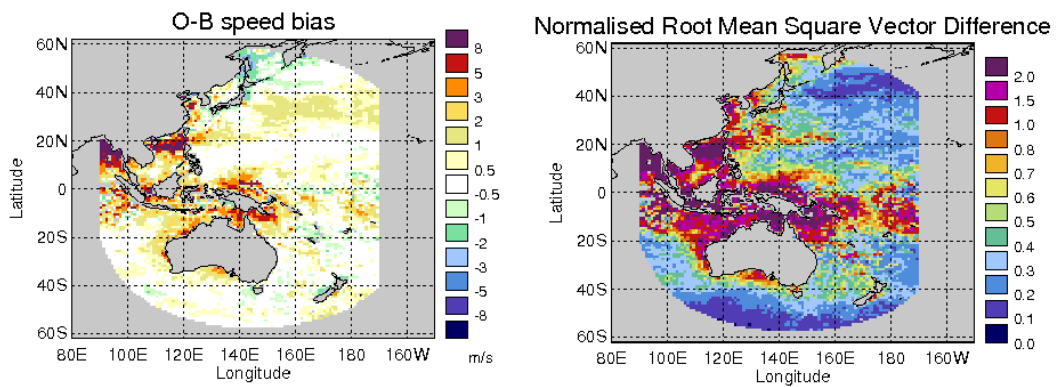
Feature Background:

Large positive O-B speed differences have been noted in previous ARs for some MTSAT and Meteosat-7 AMVs at low level. For MTSAT this was linked to height assignment error where wind shear was high, and it was noted that the problem was noticeable for IR but not VIS MTSAT AMVs.

Update:

The positive speed bias of MTSAT-2 AMVs over sea in some parts of the tropics is greatly reduced in the Himawari-8 data, along with the normalised RMSVD (Figure 1). Figure 2 shows the differences in assigned height between co-located MTSAT-2 and Himawari-8 AMVs over sea. One feature this Figure shows is that many MTSAT AMVs that were assigned heights within a band at roughly 850-900 hPa are assigned to mid or high level by Himawari-8. However, for AMVs assigned to low level in both datasets, it can be seen that Himawari-8 AMVs have lower heights on average. Although the low level Himawari-8 AMVs are not spuriously fast, Figures 3 and 2 show that a significant number have unrealistically low heights, assigned close to 1000 hPa.

Met Office: MTSAT-2 IR II, March 2016



Met Office: Himawari-8 IR II, March 2016

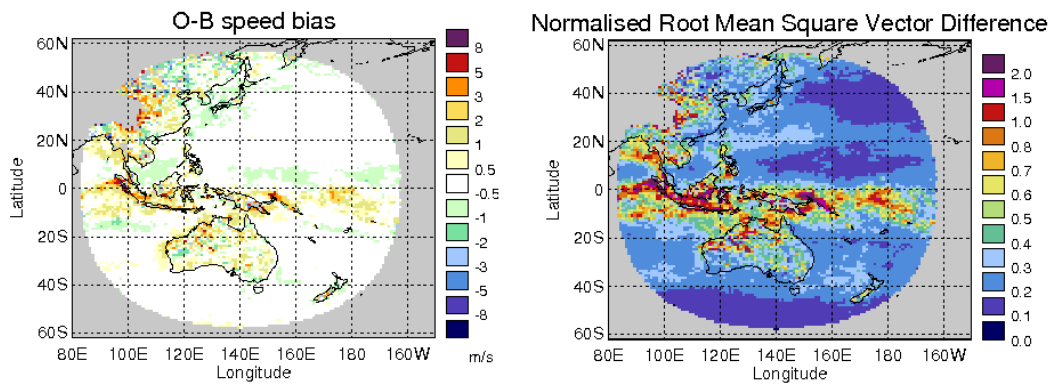
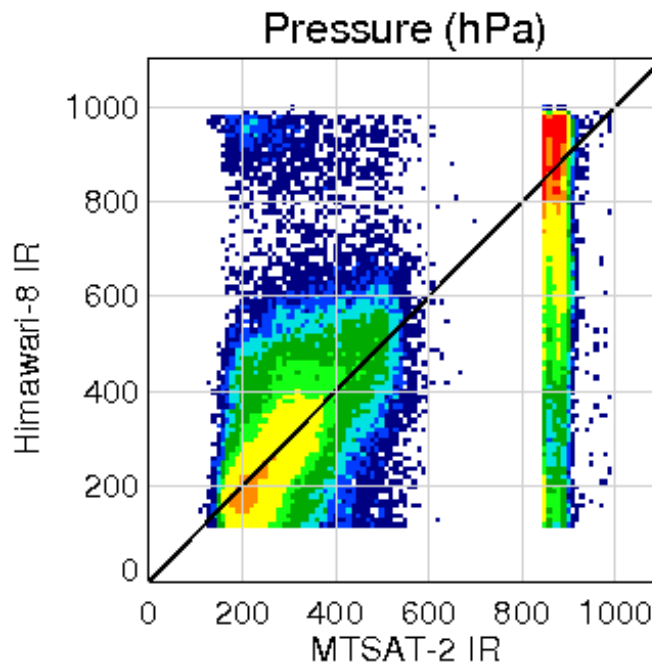


Figure 1: O-B speed bias and normalised RMSVD of MTSAT-2 and Himawari-8 AMVs, March 2016, filtered for heights below 700 hPa and QI2 > 80. Note that the MTSAT-2 AMVs were only available until 24/3/16.

Collocation Plots , March 2016



correlation coefficient = 0.894
 bias = 17.2 hPa
 rms difference = 142.8 hPa



Figure 2: Assigned heights of collocated IR AMVs from MTSAT and Himawari-8, March 2016. Filtered for QI2 > 80 and collocated within 60 minutes and 10km.

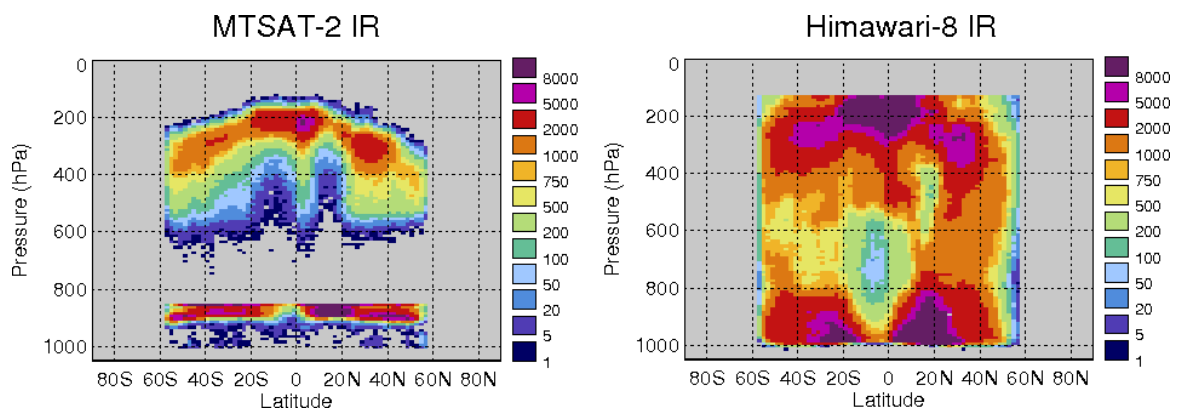


Figure 3: Zonal plots of JMA AMV data volumes for March 2016, filtered for QI2 > 80.

Met Office: INSAT-3d IR ml, March 2016

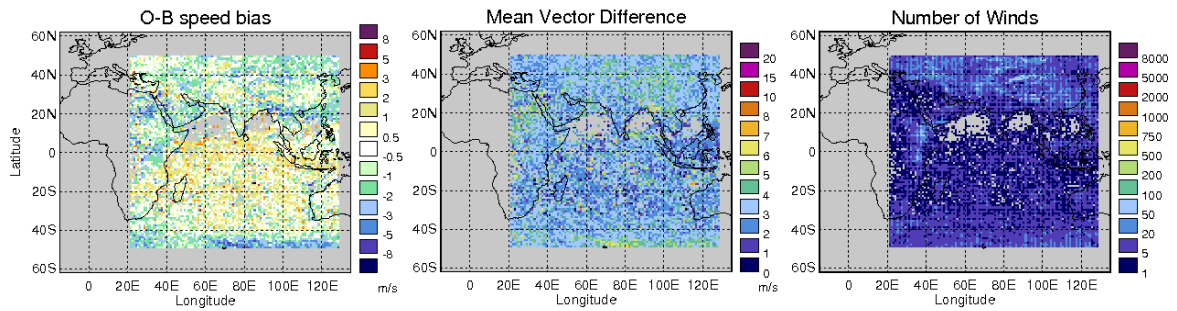


Figure 4: INSAT-3D IR AMVs, filtered for QI2 > 80 and heights between 400 and 700 hPa, March 2016.

4 Mid Level Updates

Features 2.8 and 2.9: Positive Bias in the Tropics, Negative Bias in the Extra-Tropics

Feature Background:

Previous ARs have noted that mid level AMVs tend to have a positive O-B bias in the tropics and a negative O-B bias in the extra-tropics.

Update:

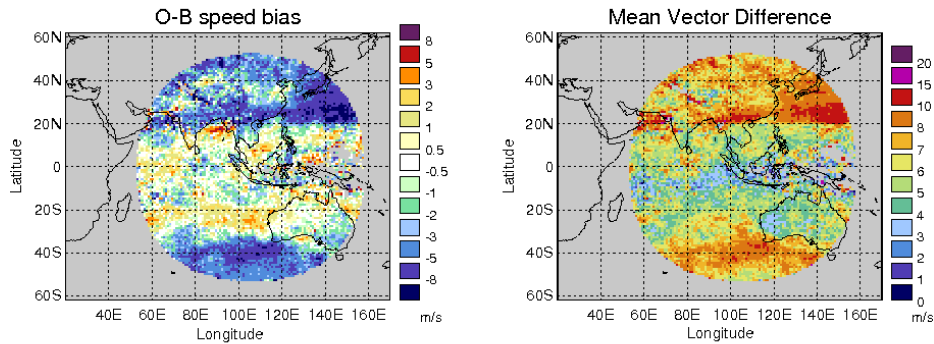
Insat-3D / Kalpana

Insat-3D AMVs were added to the NWP SAF monitoring in January 2015. At mid level, O-B speed bias and mean vector difference have been consistently low over land and sea. The number of mid level Insat-3D AMVs is small. An example month is shown in Figure 4. A significant improvement in quality but a reduction in data volume was also seen for the Kalpana AMVs since AR6.

FY-2E and FY-2G

The FY-2E AMV bias and mean vector difference were greater over the north Indian Ocean in February (Figure 5) and March 2016 than the same months in 2015. The extra-tropical FY-2E data has shown a consistent negative bias over NH land and over sea south of 40°S. O-B characteristics of FY-2G AMVs are very similar to those of FY-2E in the regions common to both satellites.

ECMWF:FY-2E-IR ml February 2015



ECMWF:FY-2E-IR ml February 2016

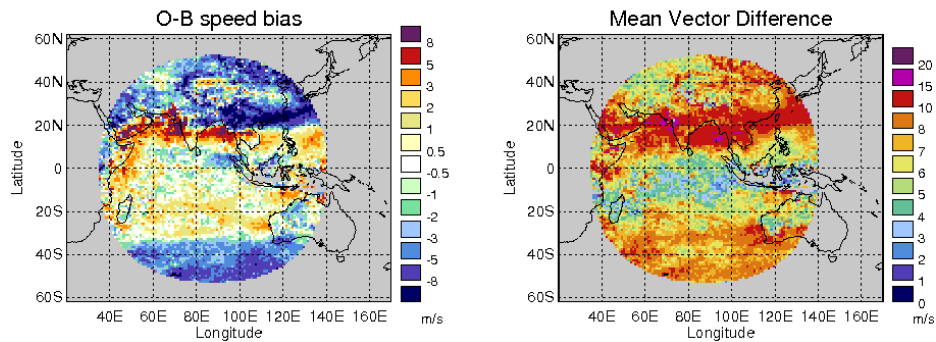


Figure 5: FY-2E IR AMVs, filtered for QI2 > 80 and heights between 400 and 700 hPa, February 2016.

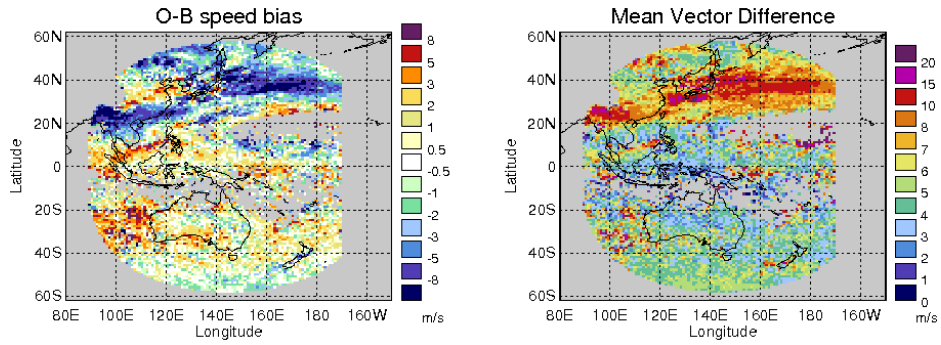
MTSAT-2 and Himawari-8

The MTSAT AMVs showed a strong negative speed bias and large mean vector difference in the northern hemisphere during winter (Figure 6). This speed bias is almost completely removed, and mean vector difference greatly reduced, in the Himawari-8 AMVs (Figure 6).

COMS-1

COMS-1 AMVs have been included in the NWP SAF monitoring since August 2015. The COMS-1 AMVs are only available in the tropics and northern hemisphere. The tropical COMS-1 AMVs consistently have a positive O-B speed bias, though it was larger in summer 2015 (Figure 7) than winter 2015/16. The NH mostly showed a positive bias in summer 2015 but a severe negative bias in winter 2015/16 with large mean vector difference.

Met Office: MTSAT-2 IR ml, January 2016



Met Office: Himawari-8 IR ml, January 2016

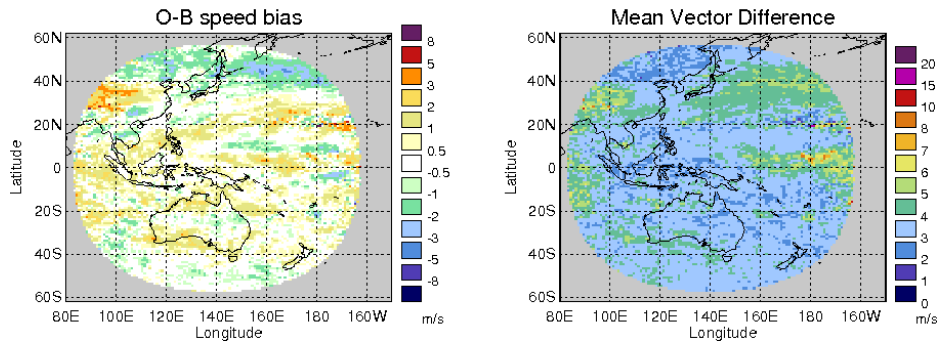
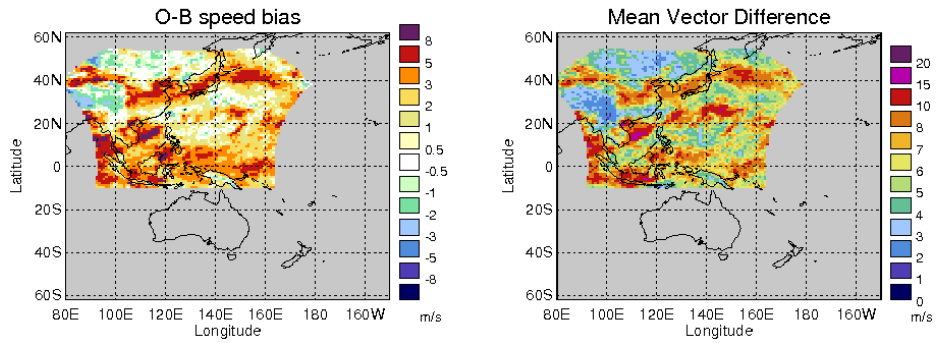


Figure 6: MTSAT-2 and Himawari-8 IR AMVs, filtered for $QI2 > 80$ and heights between 400 and 700 hPa, January 2016.

Met Office: COMS-1 IR ml, August 2015



Met Office: COMS-1 IR ml, February 2016

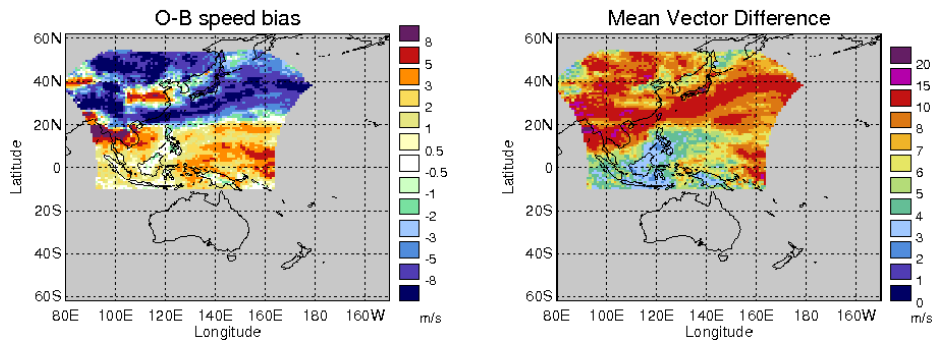


Figure 7: COMS-1 IR AMVs, filtered for $QI2 > 80$ and heights between 400 and 700 hPa.

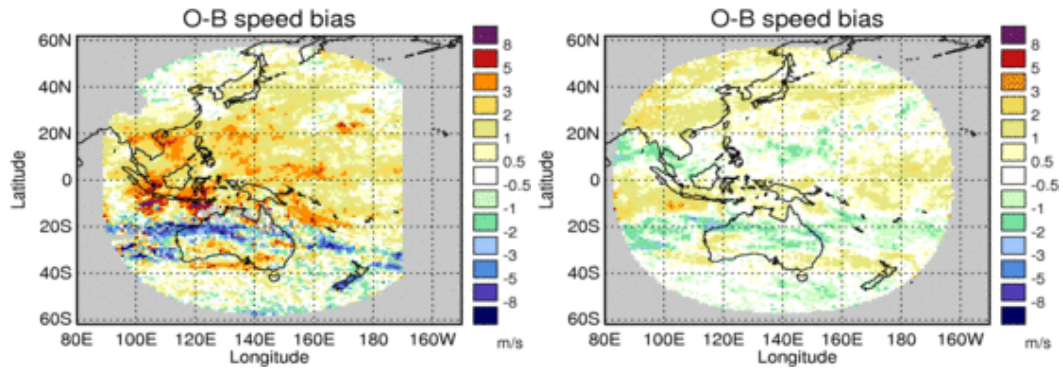


Figure 8: Mean O-B speed bias, July 2015, for MTSAT-2 WV (left) and Himawari-8 WV 6.7 (right). Observations filtered for QI2 > 80 and heights above 400 hPa.

5 High Level Updates

Feature 2.13. Tropics Positive Speed Bias

Feature Background:

Most satellite-channel combinations show a positive speed bias at high level in the tropics, particularly for the WV channels. In previous ARs, this feature has been linked to tracking and assigning heights to linear cloud tracers, and to height assignment of cloud edges in regions of wind shear.

Update:

MTSAT-2/Himawari-8

Himawari-8 AMVs have been included in the NWP SAF monitoring since July 2015. From Figure 8 it can be seen that at high level in the tropics MTSAT had a widespread positive bias, particularly large over Indonesia. Himawari-8 AMVs have a much smaller positive bias over Indonesia and small positive or negative biases elsewhere in the tropics. From the best-fit pressure statistics in Figure 9, it can be seen that the mean differences between observed and best-fit pressures are similar between the two datasets. The standard deviation of O-B pressure difference is smaller in the Himawari-8 data for high level tropics. Figures 9 and 10 both show that high level Himawari-8 AMVs are assigned higher heights than MTSAT-2 AMVs.

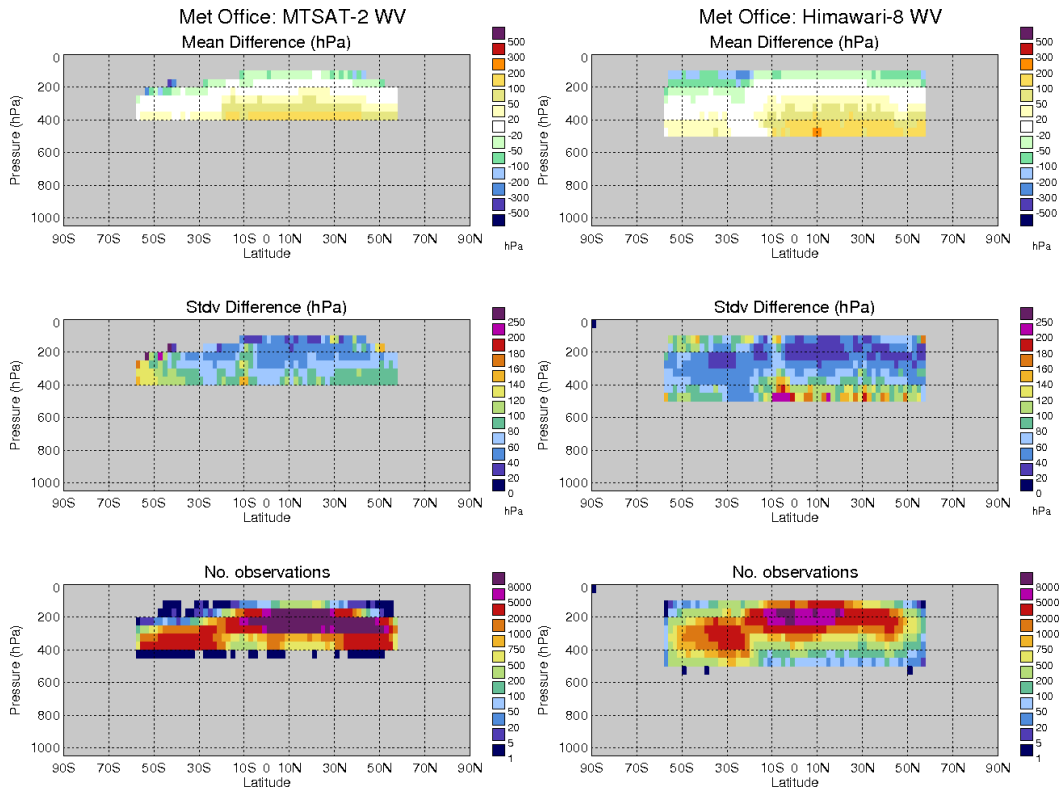


Figure 9: Best-fit pressure statistics: mean observed minus best-fit pressure differences, standard deviation of pressure differences and number of AMVs, July 2015, filtered for QI2 > 80.

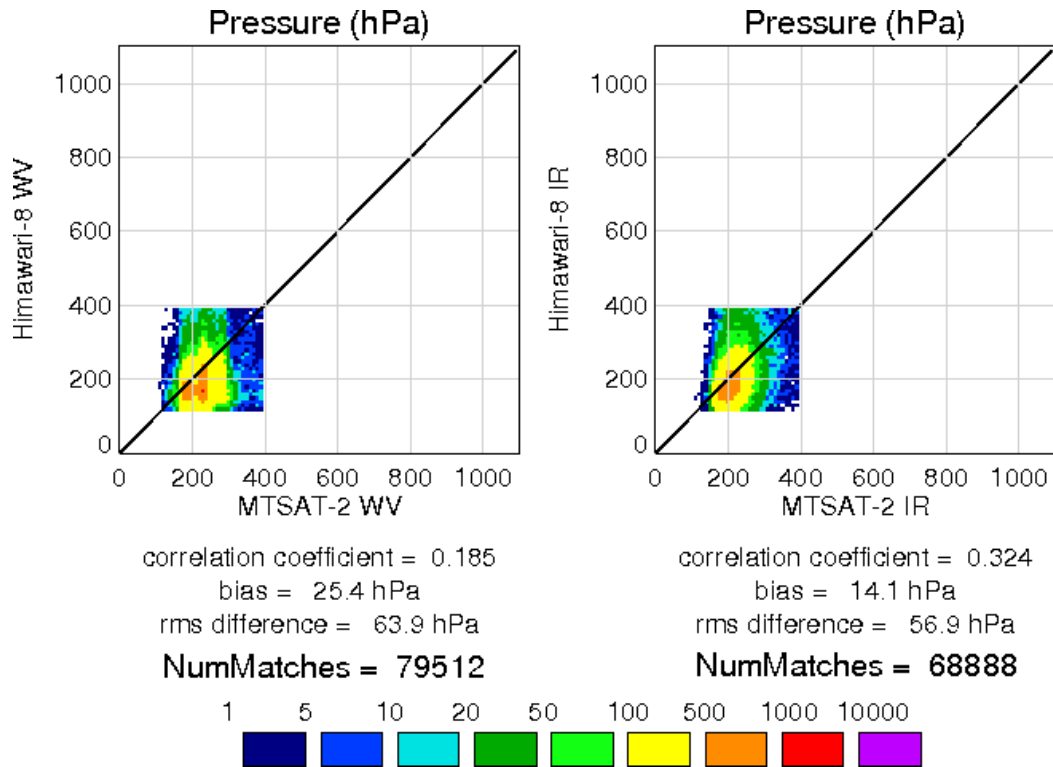


Figure 10: Himawari-8 and MTSAT-2 WV AMVs collocated within 60 minutes and 10km. Filtered for QI2 > 80, heights above 400 hPa and latitude within 20° N/S

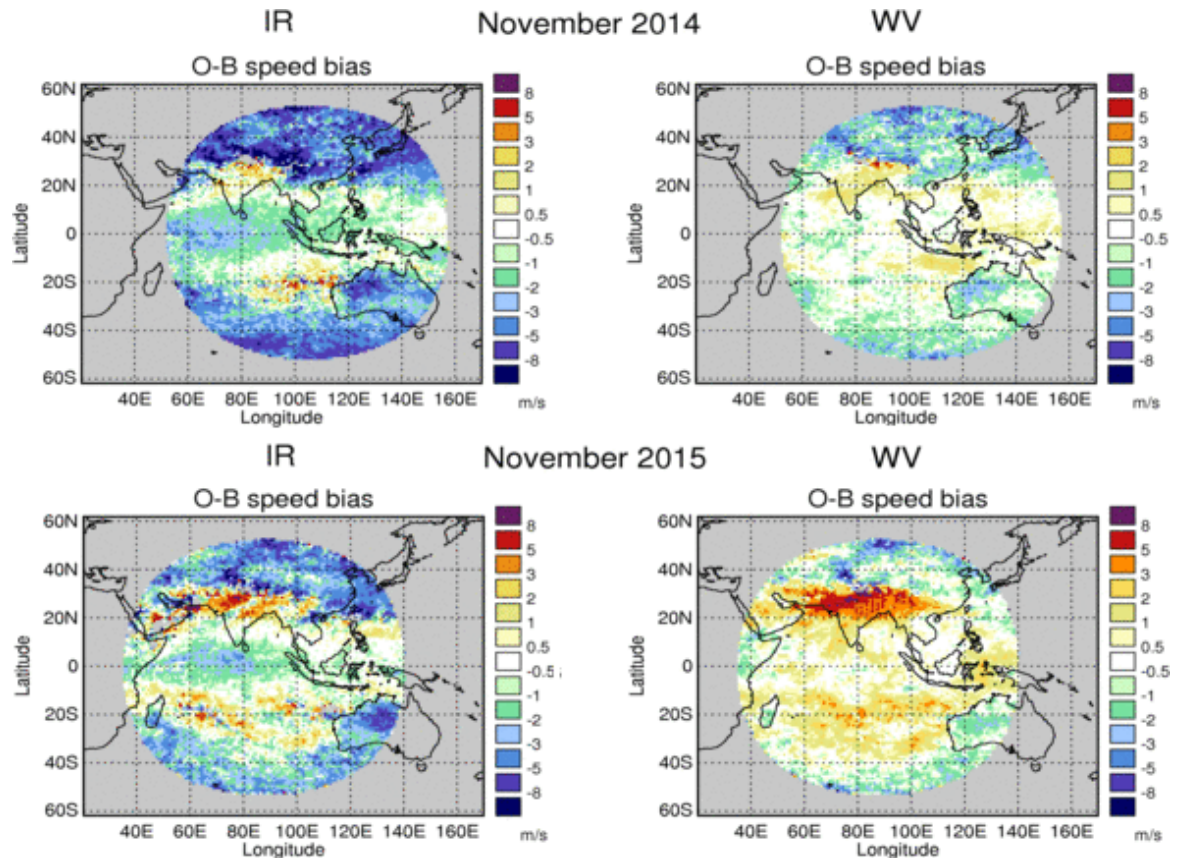


Figure 11: Difference in O-B bias of FY-2E AMVs versus ECMWF backgrounds between November 2014 and November 2015 for IR (left column) and WV (right column). Observations filtered for QI2 > 80 and heights above 400 hPa.

FY-2E/G

In AR6 it was noted that the FY-2E IR winds had a negative bias at high level in the tropics, while the WV winds were more neutral.

Derivation change:

Several updates were applied to the FY AMV derivation in late 2014 [2]. These changes seem to have led to permanent changes in the FY-2E high level tropical bias (see figure 11). The negative IR O-B bias became smaller and less widespread, while the WV O-B bias winds went from mostly neutral to a small positive bias, large over South Asia.

A possible cause of this bias change is the introduction of the 'second tracking' scheme [2]. In this scheme, tracking is done initially with a 32x32 pixel target box. Where this tracking has a high correlation coefficient (80%), the tracking is repeated with a 16x16 pixel target box. The use of smaller target boxes has previously been linked to faster AMV speeds [3]. The 16x16 wind is used instead of the 32x32 wind if the following conditions are met:

1. Correlation coefficient from 16x16 over 60%.
2. Speed calculated from 16x16 tracking is more than that of 32x32 tracking.
3. 16x16 wind direction within $\pm 60^\circ$ of 32x32 direction.

The conditions for using the 16x16 wind over the 32x32 wind would suggest that in situations where correlation coefficients are highest (i.e. tracking is easiest), faster winds are always selected. This should increase the average speed of the FY-2E winds, especially those with higher QIs, and could explain the changes seen in the biases of both AMV channels.

Separation of cloudy and clear-sky WV AMVs:

Since the 28th of January 2016 the FY-2E/G WV AMVs have been separated into cloudy and clear-sky. Figure 12 shows the change in bias of the FY-2E WV AMVs that followed the separation of cloudy and clear-sky AMVs. Most of the WV AMVs are now classified as clear-sky and show a positive O-B bias in the tropics. Of the WV winds that are classed as cloudy, most are in the tropics and have mostly neutral O-B speed bias, those outside the tropics show a negative speed bias.

Other geostationary AMV datasets have a more even split of cloudy and clear-sky winds. This is likely due to a difference in how the classification into cloudy and clear-sky is carried out. Other datasets use a cloud mask product to decide if a scene is cloudy or clear-sky. The FY-2 winds are classed as cloudy when WV brightness temperature (BT) is less than 235K and the difference between WV and IR BTs is less than 15K [2].

Feature 5.3. MTSAT Tropical Cyclone Speed Bias

Feature Background:

A positive O-B speed bias of MTSAT WV AMVs surrounding tropical cyclones was noted in AR5 [4] and AR6 [5]. In AR5 it was shown, for an example typhoon, that the MTSAT WV AMVs were on average 40 hPa below their model best-fit pressures, with the pressure difference rising to 80 hPa for WV AMVs with O-B differences greater than 8 m/s. Another typhoon case study in AR6 showed similar O-Bs.

Update:

Typhoon Dujan of 19th-30th September 2015 developed a well defined eye, shown in Figure 13. Himawari-8 is higher resolution than MTSAT. The Himawari-8 AMVs also have a new derivation scheme which mixes the benefits of tracking fine detail with a small tracking box with the reliability

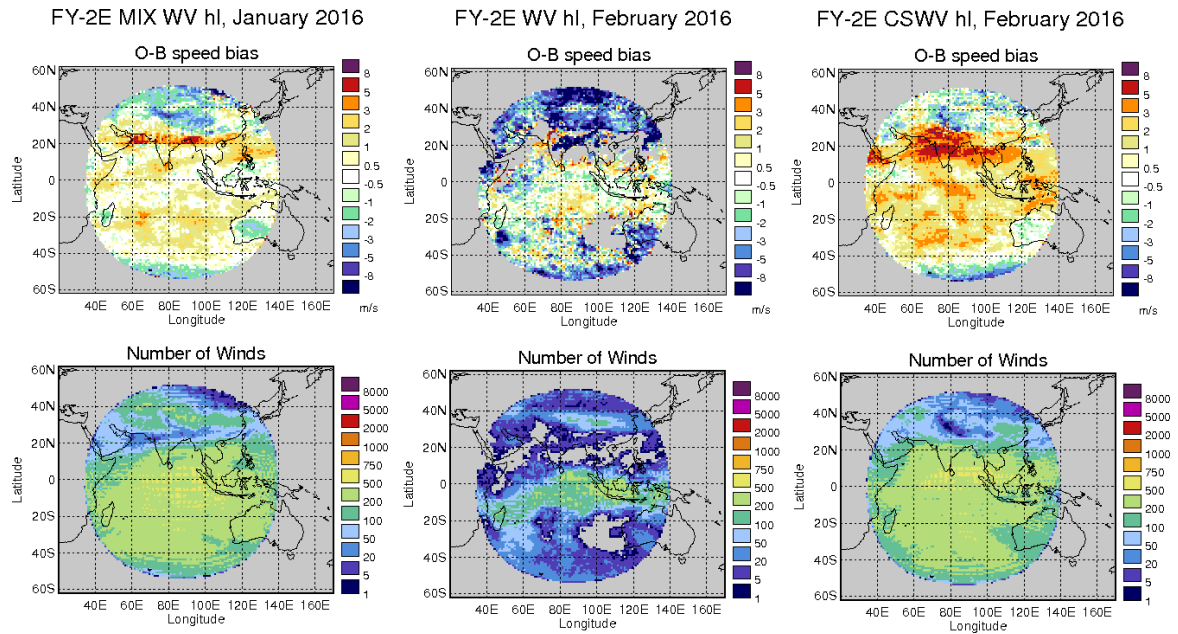


Figure 12: Change in FY-2E O-Bs from mixed WV winds in January 2016 (left column) to cloudy WV winds (middle column) and clear-sky WV winds (right column) in February 2016. Winds filtered for $QI2 > 80$ and heights above 400 hPa.

that comes with the use of a larger target box[1]. These two differences help explain the difference in the volume and coverage of AMVs shown in Figure 14. The Himawari-8 AMVs are more numerous and are extracted closer to the eye of the typhoon.

By inspecting Figure 15, we can see that where WV AMVs are extracted for both satellites, the Himawari-8 speed differences tend to be lower than those of MTSAT-2. For example, over sea to the south of the Philippines, the MTSAT AMVs mostly have large positive speed differences, which is not the case for Himawari-8 WV AMVs at the same locations. The Himawari-8 AMVs derived near to the southeast of the typhoon eye have large positive speed differences, others near the eye have a mix of positive and negative differences. O-Bs for Typhoon Krovanh during 16-17 September 2015 were similar in that Himawari-8 AMVs had smaller O-B speed differences than co-located MTSAT AMVs, however the Himawari-8 AMVs near the eye showed a mix of O-B differences with no clear pattern.

Feature 6.3. Very High FY-2E WV Winds

Feature Background:

AR6 noted some FY-2E mixed WV channel winds assigned unrealistically high in the atmosphere, particularly in the winter hemisphere, some with pressures as low as 0 hPa.

MTSAT2 10.8 μ m IR 25/09/2015 1800 UTC

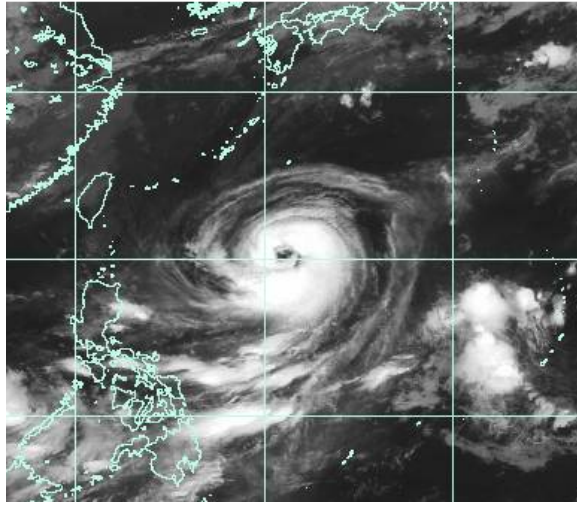


Figure 13: Himawari-8 IR imagery of Typhoon Dujan, 25/9/15, 18UTC.

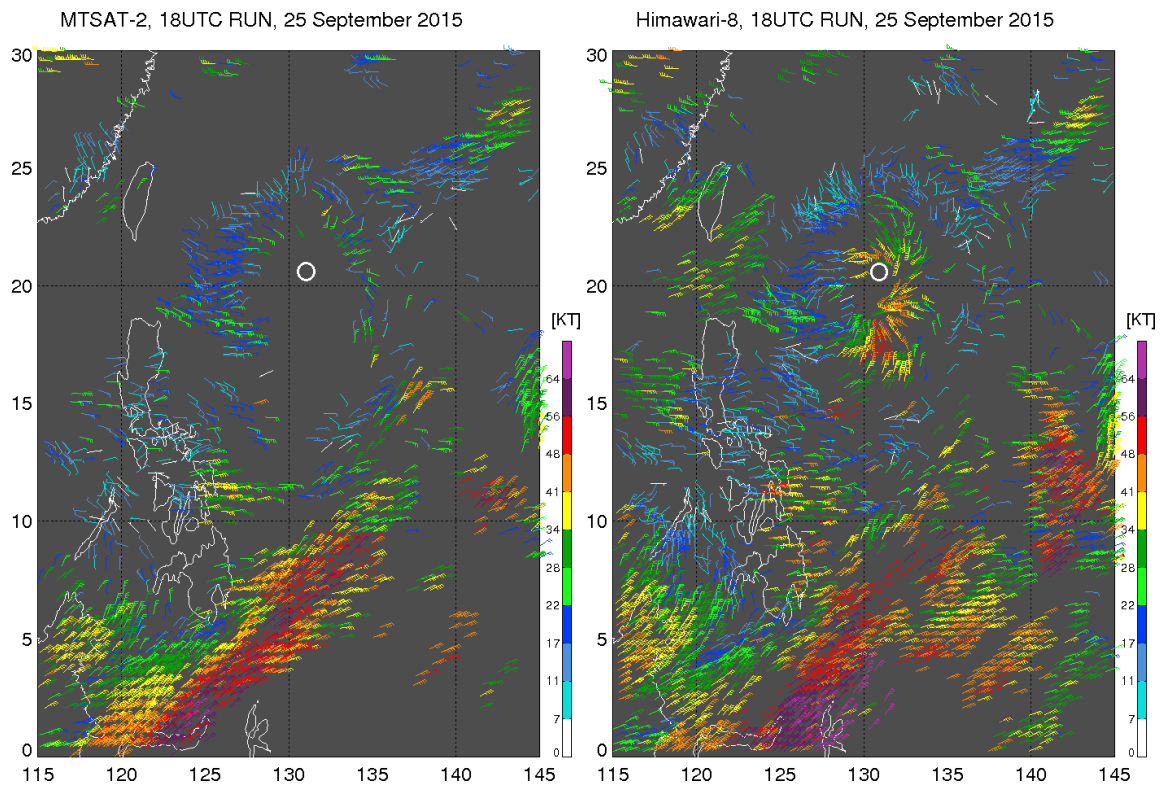


Figure 14: JMA AMVs between 1500 to 2100 UTC, 25/9/15, WV 6.7 micron channel.

O-B Speed Difference, MTSAT-2, 18UTC RUN, 25 September 2015 O-B Speed Difference, Himawari-8, 18UTC RUN, 25 September 2015

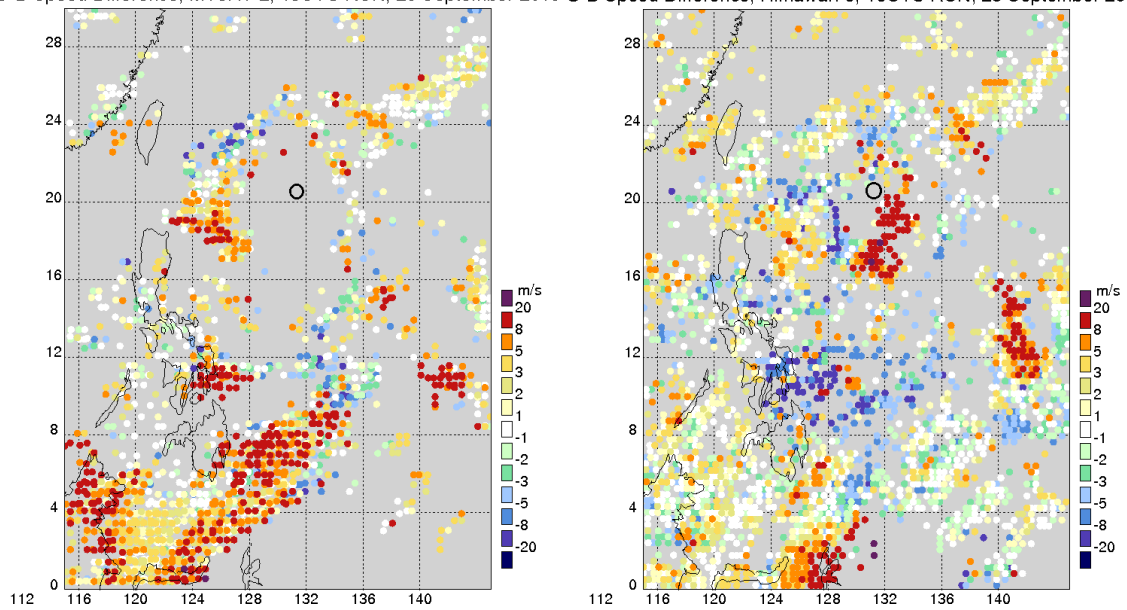


Figure 15: O-B speed differences of JMA WV (6.7 micron) AMVs between 1500 to 2100 UTC, 25/9/15.

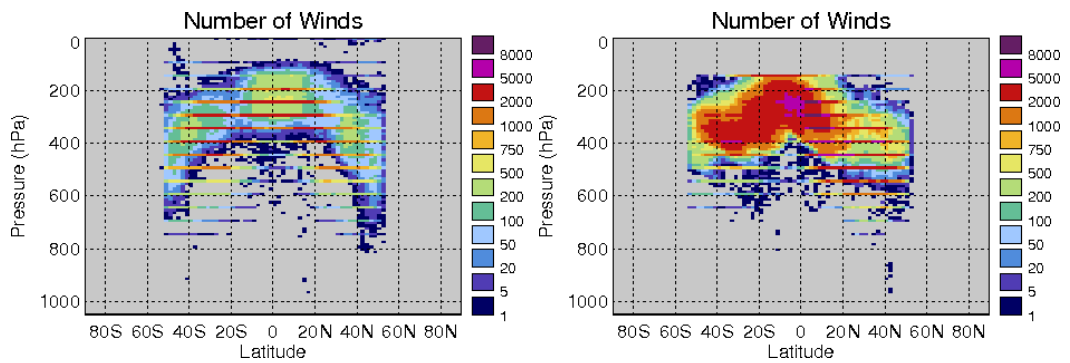


Figure 16: Zonal distribution of FY-2E winds for November 2014 (left) and January 2015 (right). Observations filtered for QI2 > 80.

Update:

The FY-2E derivation scheme was updated in December 2014. Following the change the FY-2E winds appear to be capped around 150 hPa (Figure 16). This cap is also in place for the FY-2G winds which were added to the monitoring in July 2015. The pressure level clustering noted in AR6 is still present in both the FY-2E and FY-2G WV winds.

Met Office: Dual Metop IR 10.8 hl, March 2016

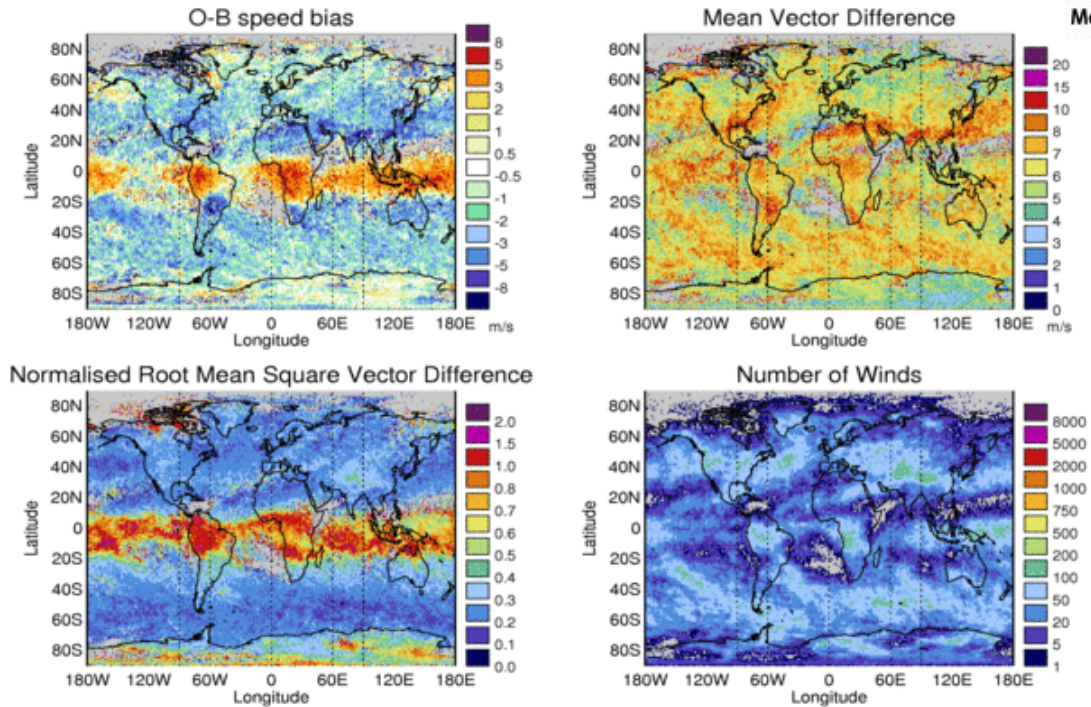


Figure 17: Dual-Metop O-Bs versus Met Office backgrounds, March 2016, filtered for heights above 400 hPa and for Q12 > 80.

6 Polar Wind Updates

Feature 7.1. Dual-Metop Positive Bias in Tropics

New Feature:

The Dual-Metop AMVs, included in the NWP SAF monitoring since September 2014, consistently show a positive O-B speed bias in the tropics. This positive bias is particularly large at high level, and can be seen in Figure 17, along with the high normalised RMSVD in the tropics. The widespread nature of the positive bias, which occurs over sea and land, and which occurs over the Inter-Tropical Convergence Zone (ITCZ), an area where tall cumulonimbus clouds are common, suggests a problem with image geometry.

Figure 18 shows Dual-Metop satellite zenith angles (SZAs) and O-B speed differences over the Mid-Atlantic on 15th of March 2016. The SZA is that of the first image of the two used for deriving an AMV. From the speed difference plot, it can be seen that generally, in the region of the ITCZ, high first image SZA correlates with smaller O-B speed differences.

The relation between a month of Dual-Metop O-Bs and their SZAs is shown in Figure 19. The top two rows show there is a small variation in bias and very little change in RMSVD with SZA for extra-tropical Dual-Metop AMVs. The third row shows that at high level in the tropics, RMSVD and positive O-B bias reduce with increasing SZA. The fourth row shows that at tropical high level the correlation is stronger - there is a drop of approximately 3 m/s each in bias and RMSVD as SZA increases from 0 to 60 degrees. Figure 20 maps the difference in O-B speed bias and normalised RMSVD between high- and low-SZA Dual-Metop AMVs. It can be seen that speed bias and RMSVD are reduced, though still apparent, for the high-SZA Dual-Metop AMVs.

In the tropics, just the edges of consecutive Metop swaths overlap, not the full swath. So if the SZA of the first image is high, the SZA of the second image is low, and vice versa. The strong correlation between the bias and RMSVD with SZA of tropical Dual-Metop AMVs may be because the Dual-Metop AMVs are assigned their height from the second image of the pair (O. Hauteceur, pers comm., Apr 2016). This helps explain the relation seen in Figure 19, as it suggests that AMV quality suffers when the height assignment is done from a high SZA. For AMVs with a lower SZA in their first image than their second image, more accurate height assignment may be possible if the first image is used for height assignment rather than the second.

If improved HA involved a lowering of the heights of tropical Dual-Metop AMVs, Figure 21 suggests that this could reduce the positive O-B speed bias of these AMVs at high level. It shows that a large proportion of tropical Dual-Metop AMVs are assigned to roughly 200 hPa. At this height they have an average speed of roughly 14 m/s but Met Office global model backgrounds average 13 m/s. The model background averages 14 m/s at around 300 hPa.

Feature 7.2. EUMETSAT Metop High Level Negative Bias in Extra-Tropics

New Feature:

Following derivation updates in May 2014, the overall O-Bs of EUMETSAT Single-Metop AMVs improved substantially. However, the high level slow bias that was present for a small number of EUMETSAT Metop AMVs before the derivation update became larger and more extensive following the update (see June O-Bs in Figure 22). When the Dual-Metop AMVs were added to the NWP SAF monitoring in September 2014 the high level slow bias was also present throughout the rest of the extra-tropics. This extra-tropical high level slow bias is in contrast to other polar AMVs for which a slight positive high level bias has been documented in ARs 2-5.

Satellite Zenith Angle, Dual Metop, 12UTC RUN, 15 March 2016 O-B Speed Difference, Dual Metop, 12UTC RUN, 15 March 2016

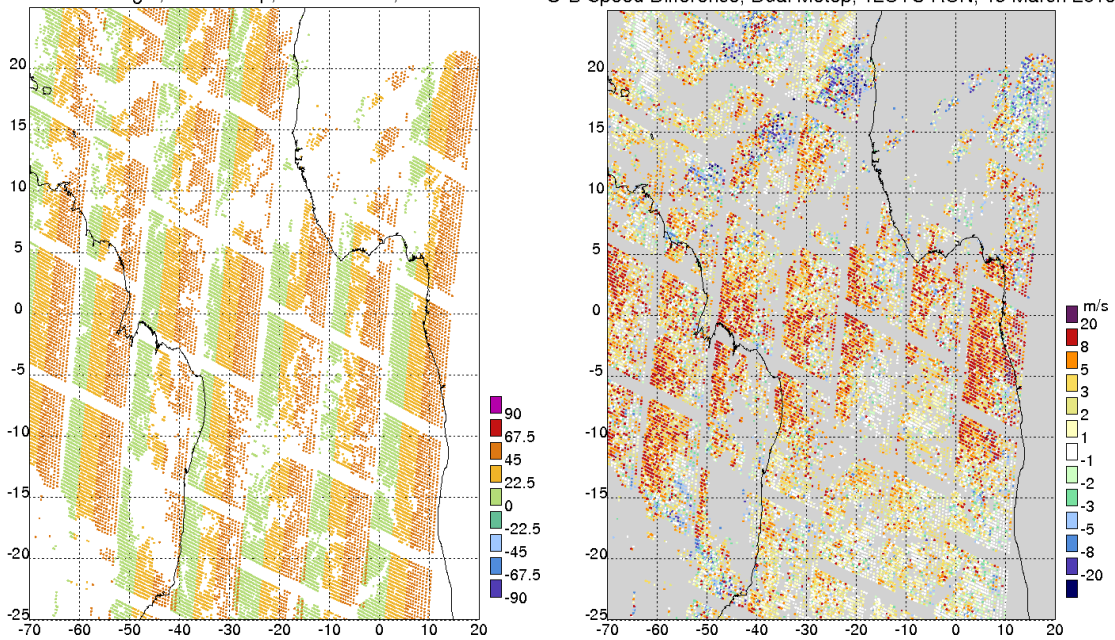


Figure 18: Properties of Dual-Metop AMVs from 0900 to 1500 UTC, 15/3/16.

Feature 7.3 MISR Fast Bias over Ice and Desert

New Feature:

MISR O-B monitoring often shows a positive speed bias and large mean vector difference at low level over ice and desert (see example in Figure 23).

In Figure 24, there are some MISR winds clustered around 20N, 5W with a range of speeds but all in a westerly or west-by-southwesterly direction. From Figure 25 it can be seen that Meteosat-10 infra-red imagery shows clouds moving in the same direction as the MISR vectors.

The Meteosat-10 cloud product gives cloud-top-heights (CTHs) for these clouds of at least 12km (Figure 26). However, the MISR vectors' heights are much lower in the atmosphere (Figure 27), close to the surface. This leads to a large positive O-B bias (Figure 27) since the UKMO model winds are much stronger at high level where the clouds are than near the surface where the MISR winds are (Figure 28).

The reason for the low heights assigned to the MISR vectors is believed to be due to tracking cloud shadows rather than the clouds themselves (K. Mueller, pers comm., Apr 2016). Over bright surfaces such as desert and ice, the contrast between the cloud shadows and the surface is greater

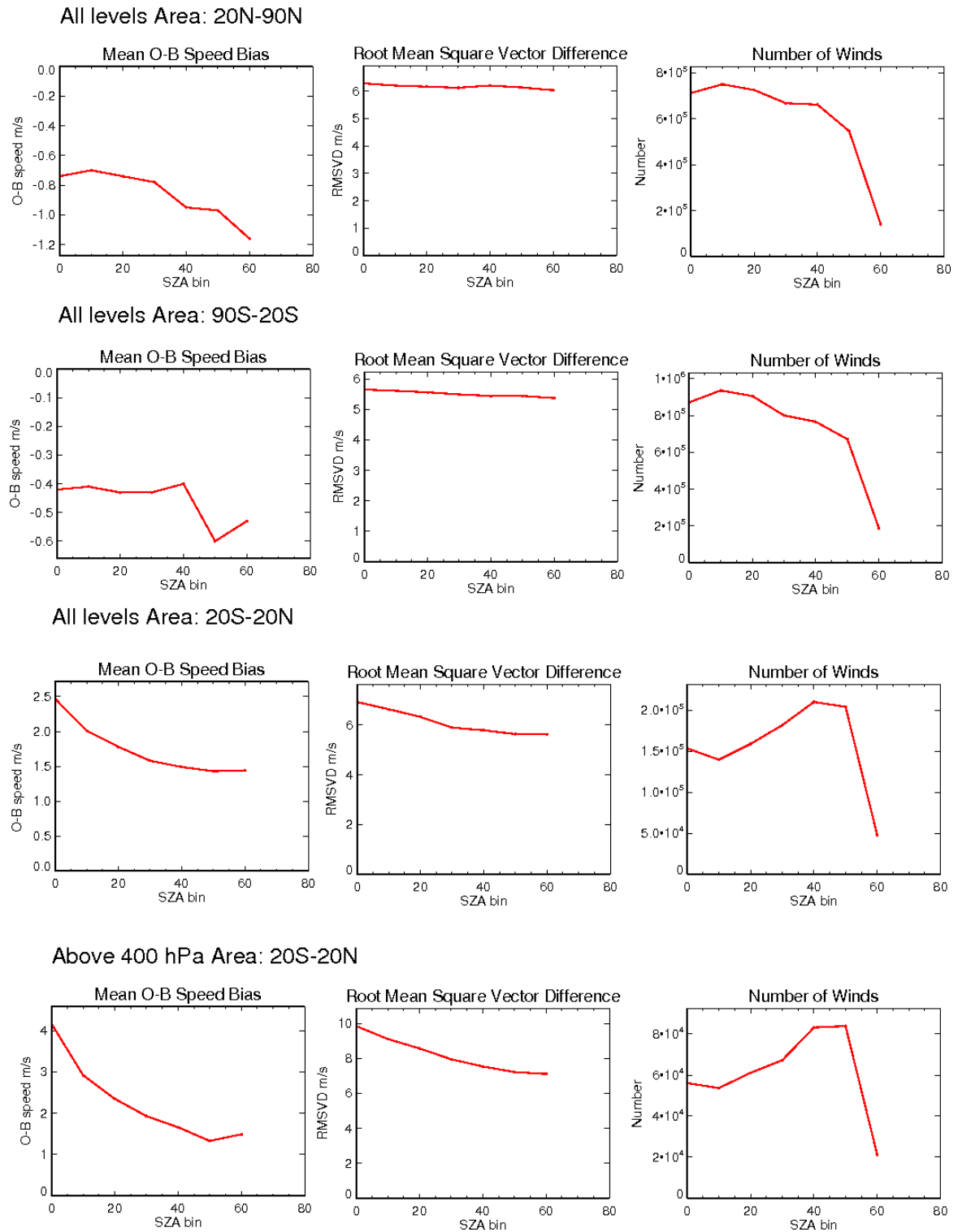


Figure 19: Change in Dual-Metop O-Bs and data volumes with SZA for March 2016, versus Met Office backgrounds, filtered for QI2 > 80. Note the variation in y-axis scale.

Met Office: Dual Metop IR 10.8 hl, March 2016

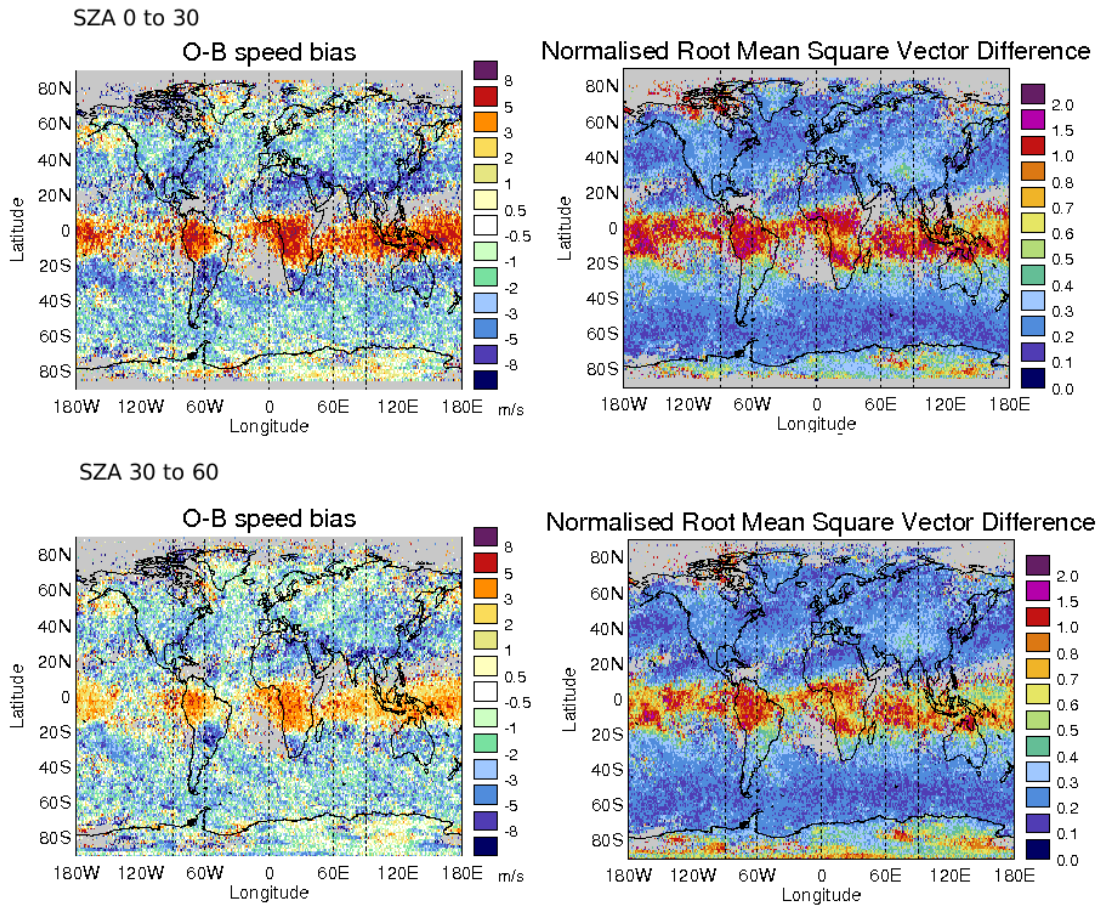


Figure 20: O-B speed bias and normalised RMSVD of March 2016 Dual-Metop AMVs, filtered for QI2 > 80 and heights above 400 hPa. Top row: satellite zenith angle of first image in range 0° to 30°, bottom row: satellite zenith angle of first image in range 30° to 80°.

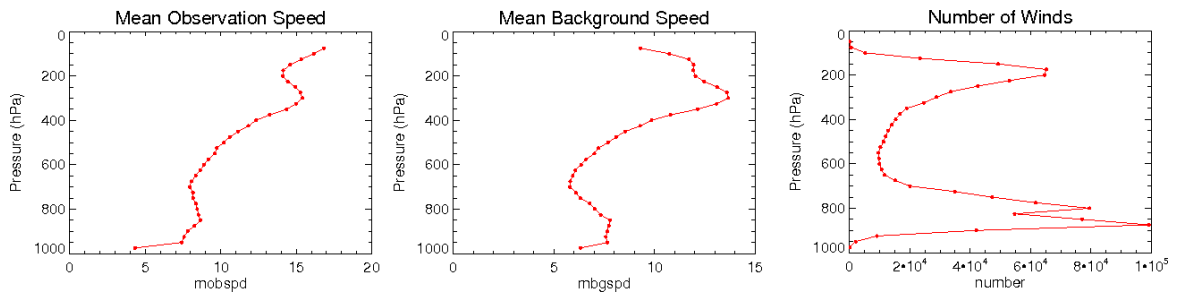
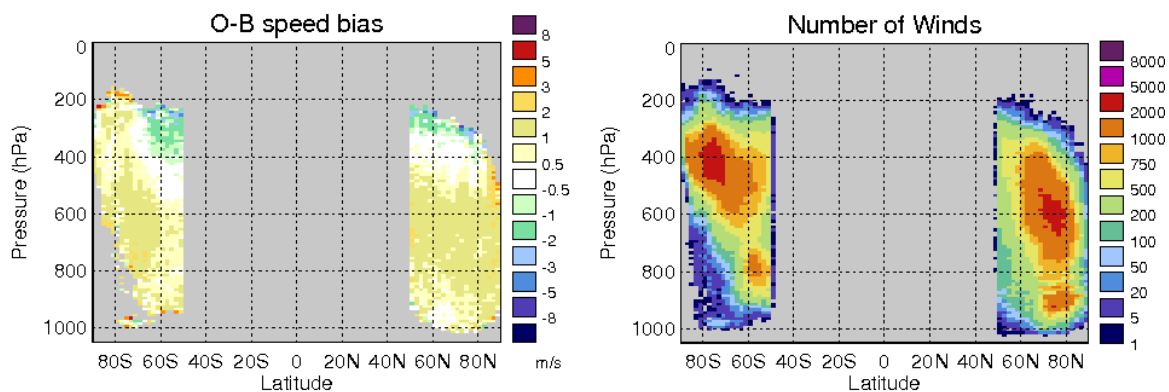
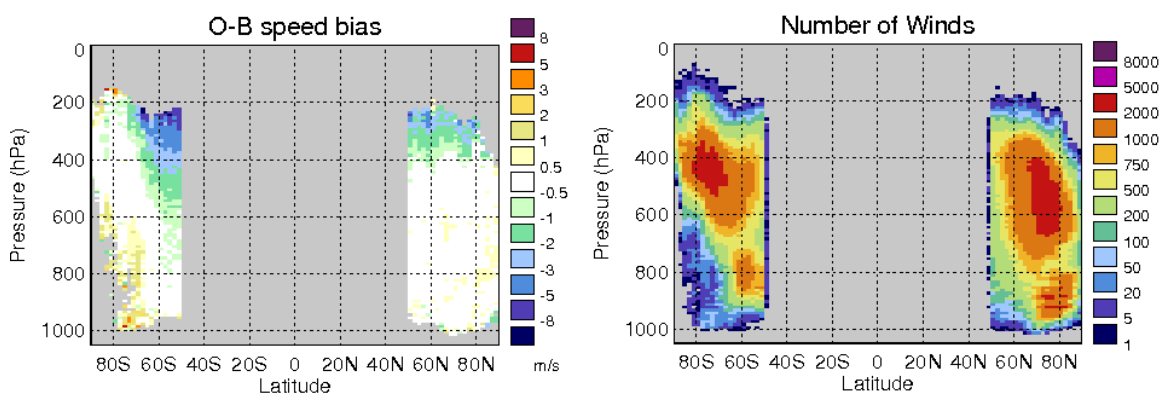


Figure 21: Dual-Metop O-Bs' variation with pressure, calculated against Met Office backgrounds, March 2016. Filtered for QI2 > 80 and latitude within 20° N/S.

Met Office: EUMETSAT Metop-B IR 10.8, May 2014



Met Office: EUMETSAT Metop-B IR 10.8, June 2014



Met Office: Dual Metop IR 10.8, September 2014

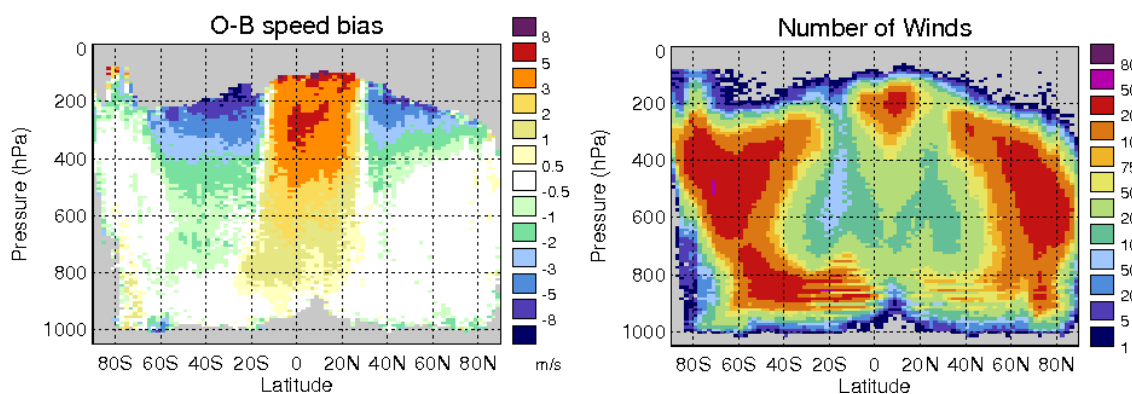


Figure 22: Zonal plots of O-B speed bias and data volume for EUMETSAT's Single and Dual AMV products. Single-Metop filtered for $QI2 > 60$, Dual-Metop filtered for $QI2 > 80$.

Met Office: MISR StereoMV VIS 0.6 II, August 2015

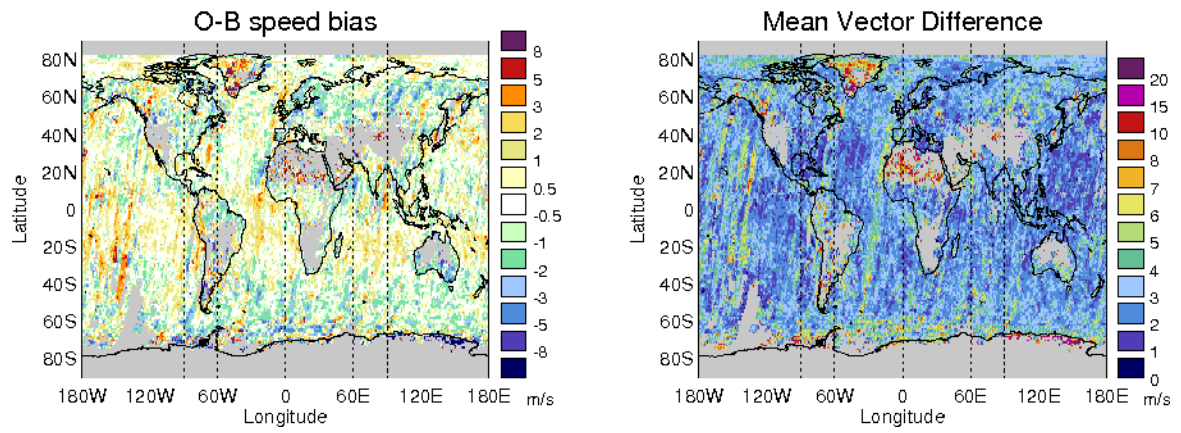


Figure 23: O-B bias and mean vector difference of MISR winds, August 2015. filtered for QI2 > 80 and heights below 700 hPa.

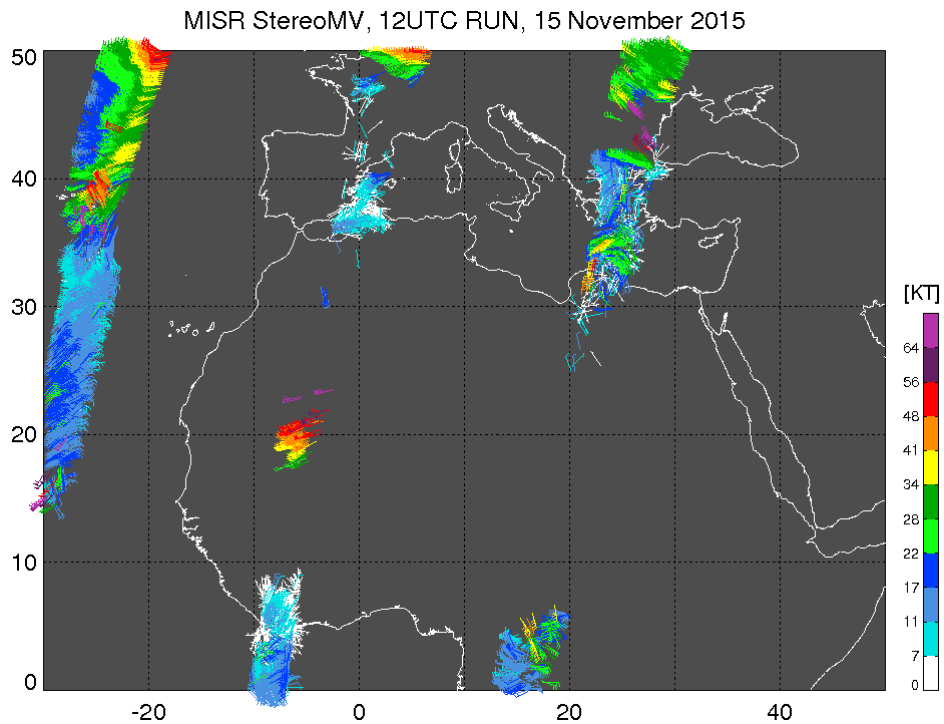


Figure 24: MISR wind vectors received at the Met Office in time for the 12UTC data assimilation run, 15th November 2015.

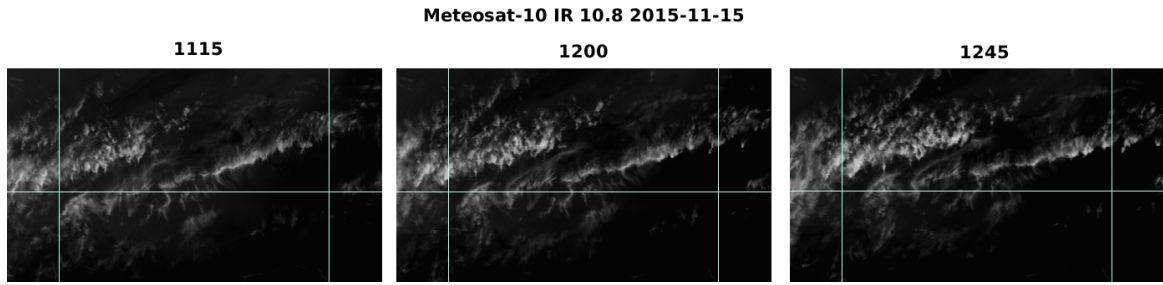


Figure 25: Meteosat-10 IR 10.8 image sequence from 15th of November 2015 showing eastward cloud motion.

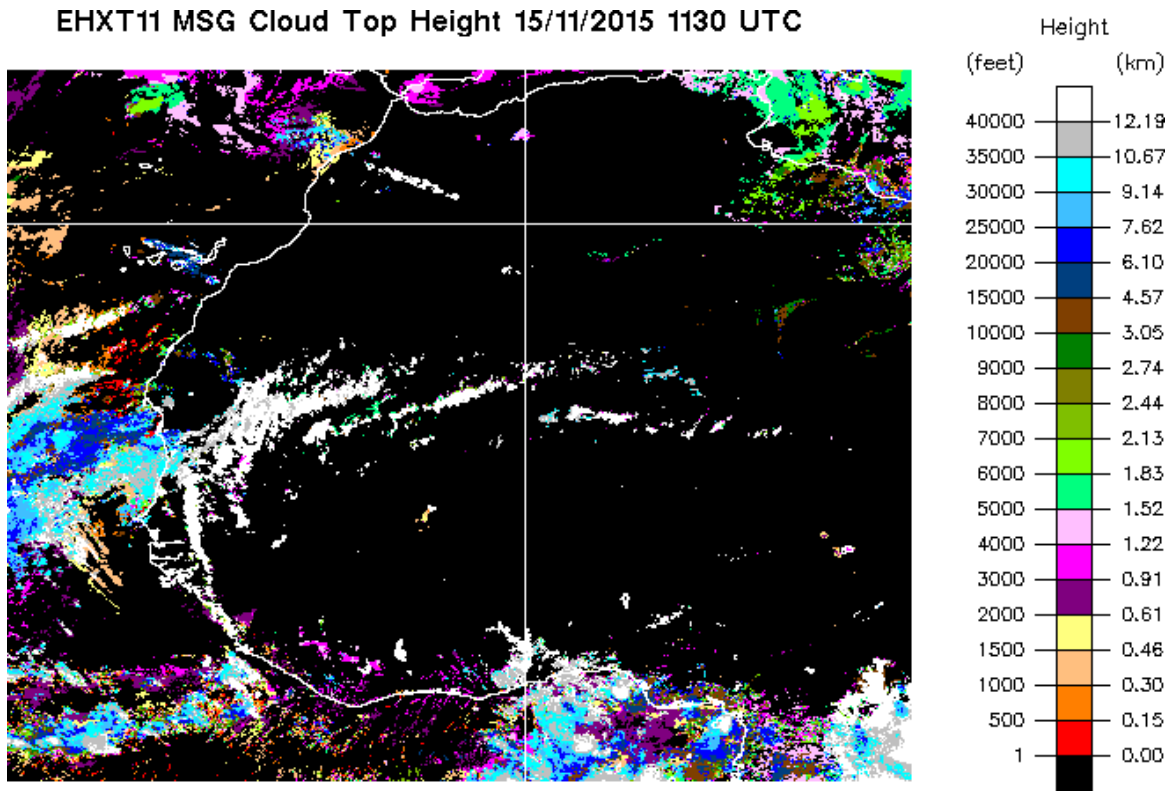


Figure 26: Meteosat-10 cloud top heights.

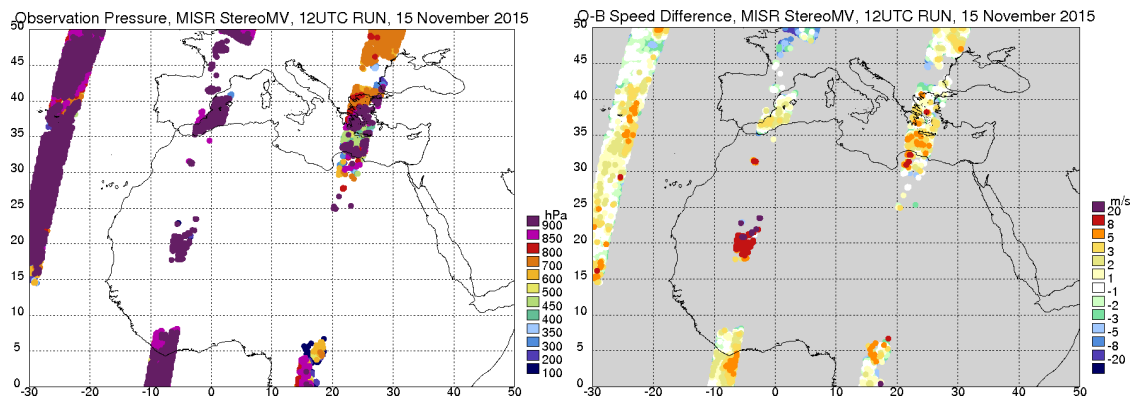


Figure 27: Left: Heights of MISR vectors. Right: O-B speed differences of MISR vectors.

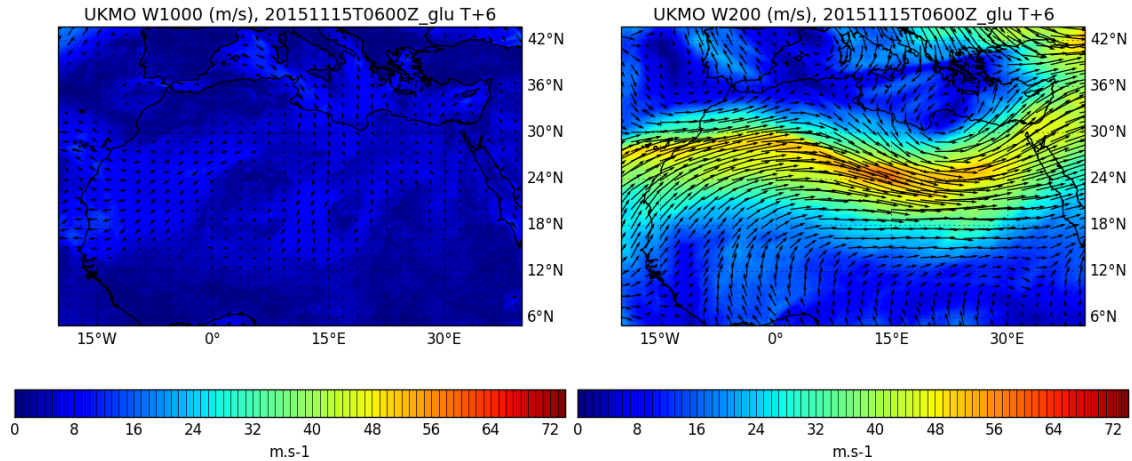


Figure 28: UKMO model background winds valid at 12UTC, 15th November 2015. Left: winds at 1000 hPa. Right: winds at 200 hPa.

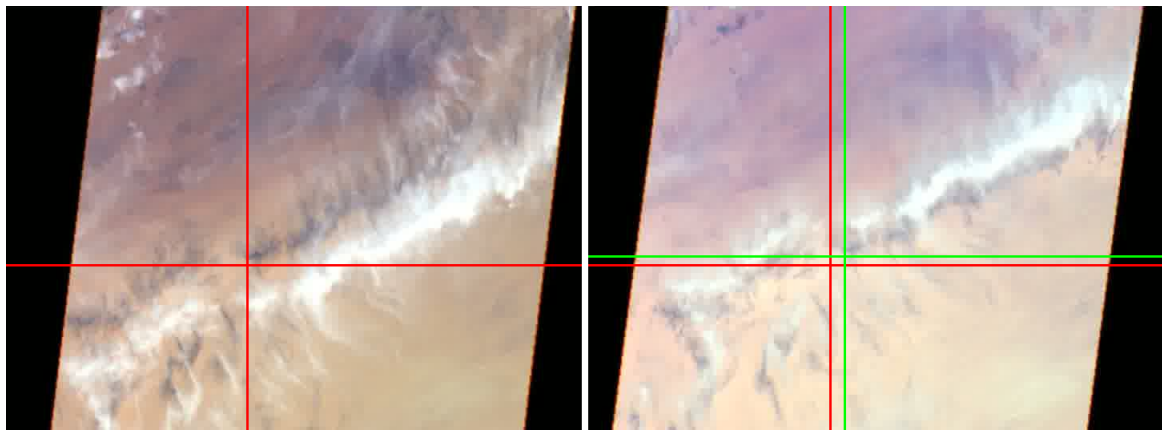


Figure 29: MISR true colour imagery at the time and location of the case study. Left: 70° forward camera. Right: 70° aft camera. The crosses mark the south-west edge of one cloud feature's shadow as an example. The red cross is the location in the forward view, the green cross is the location in the aft view.

than that between clouds and the surface. If the cloud shadows are moving fast enough, then they avoid being marked as stationary surface features, and are tracked as tracers. Since the shadows have no apparent north-south motion due to parallax as is seen for clouds, they are assigned heights very close to the surface. Figure 29 shows an example of a moving shadow for this case study.

Feature 7.4 LeoGeo Coverage Gaps at Particular Longitudes

New Feature:

Monitoring of the LeoGeo AMVs, which are derived using imagery from a mix of geostationary and

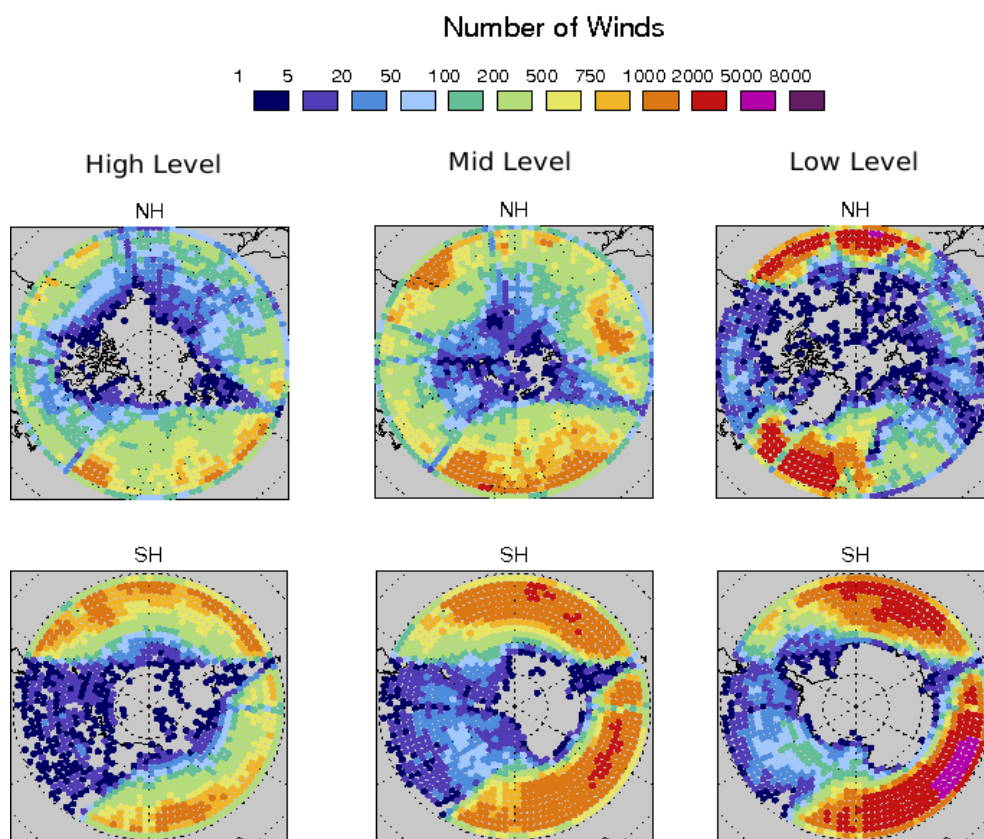


Figure 30: Map of LeoGeo AMV data volumes, filtered for $QI2 > 80$, and for heights above 400 hPa (left), between 400 and 700 hPa (middle) and below 700 hPa (right).

polar satellites, consistently shows low observation counts at particular longitudes. The longitudes can be seen in the standard NWPSAF plots in Figure 30, but are more clear when the data is shown on a global projection (Figure 31). The longitudes with little or no data are at roughly 90°W , 75°E and 90°E (both hemispheres), and 170°W , 105°W , 35°W (northern hemisphere only).

Feature 7.5 Stripes of Large O-Bs in MISR Data.

New Feature:

Monitoring of MISR AMVs often reveals stripes of data with large O-B differences (see example in Figure 32). These are usually over the Atlantic or Pacific oceans.

MISR winds retrieval requires visible landmarks to calibrate its camera geometry. The near-real-time MISR winds processing is done with 10-50 minute data sessions. A session's data quality can be degraded if the Terra satellite does not pass over enough land to calibrate its cameras during

Met Office: CIMSS LeoGeo IR AllLev, March 2016

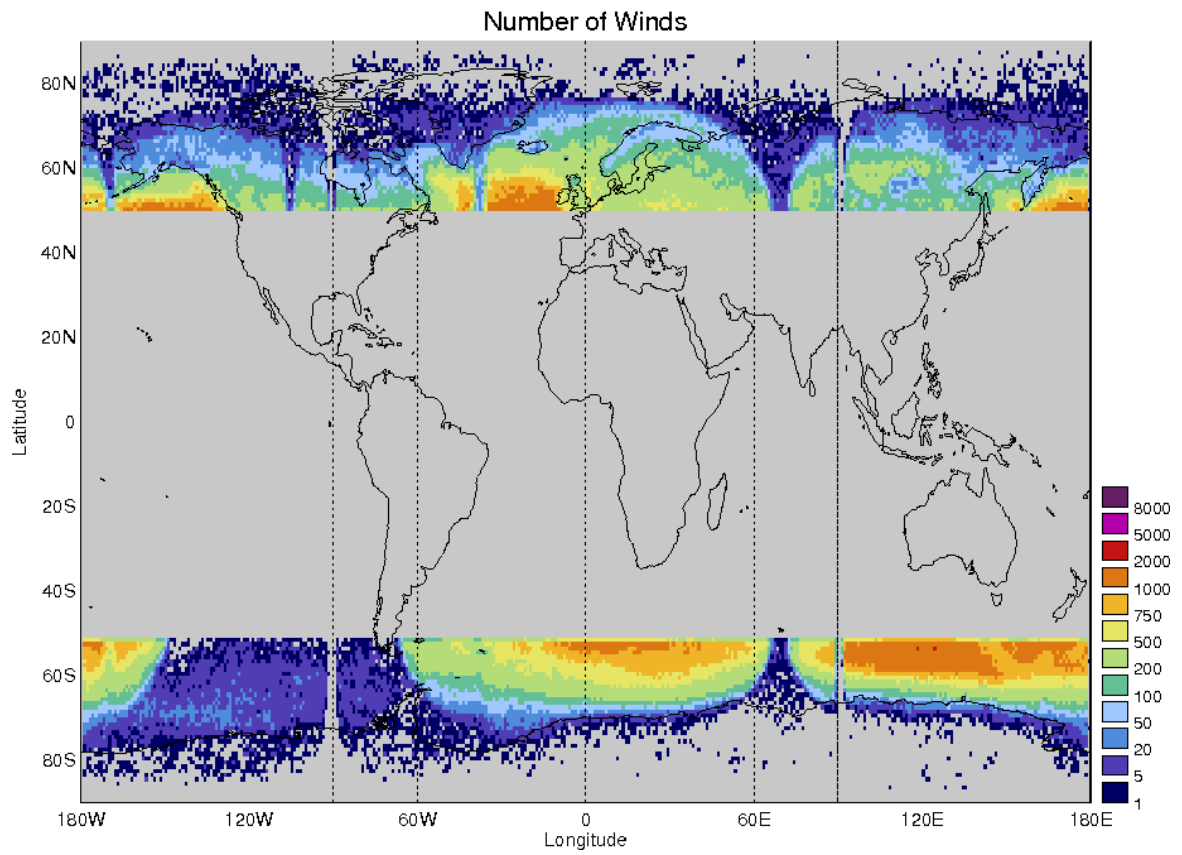


Figure 31: Map of LeoGeo AMV data volume, March 2016, all heights, filtered for $QI_2 > 80$

Met Office: MISR StereoMV VIS 0.6 II, August 2015

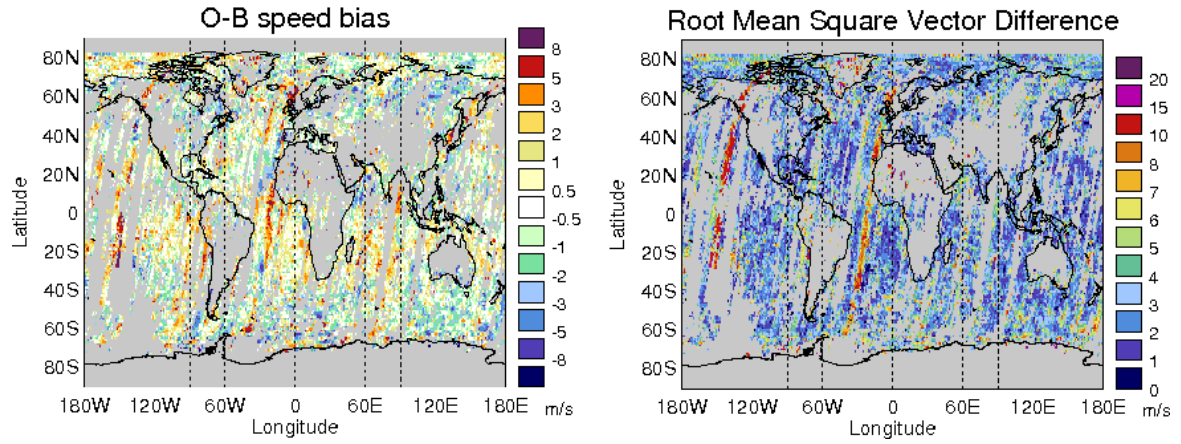


Figure 32: Speed bias and RMSVD of MISR AMVs, 17th-24th August 2015. Filtered for heights below 700 hPa.

that session (K. Mueller, pers comm., May 2015).

This feature was more prominent from the start of monitoring in May 2015 until October 2015 than in the months since November 2015.

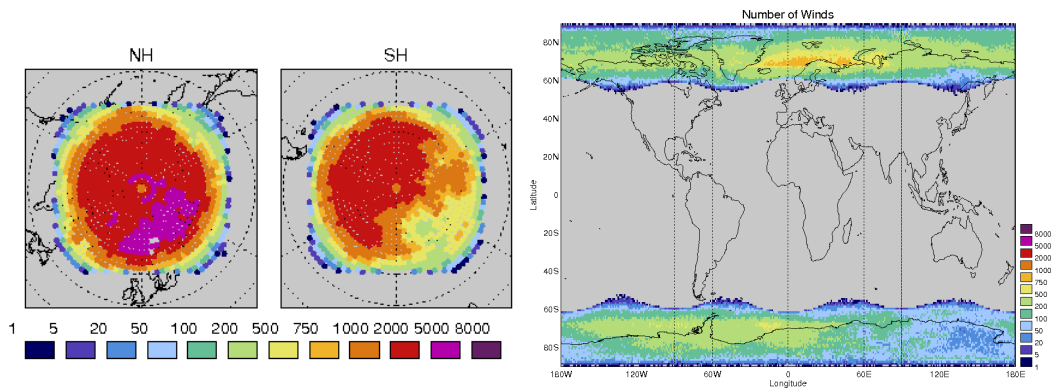


Figure 33: Spatial distribution of Suomi-NPP VIIRS winds, all height levels, September to December 2015.

Feature 7.6. Square-Shaped Spatial Distribution of Suomi-NPP Winds

New Feature:

The Suomi-NPP VIIRS winds, monitored since February 2015, have an unusual spatial distribution, which appears square-shaped on a polar projection (Figure 33). The right panel of that Figure shows the winds plotted on a global projection and the square shape of the distribution is revealed by the four spikes in the coverage pattern for each hemisphere. The cause of the square distribution is known to be the dimensions of a box used for the polar projection during the derivation process (J. Key and D. Santek, pers comm., July 2015).

7 Summary

NWP SAF monitoring of AMVs remains useful for understanding sources of AMV error. Since AR6 new AMV datasets have been added to the monitoring including Dual-Metop, INSAT-3D, Suomi-NPP, MISR, Himawari-8, COMS-1 and FY-2G.

The most significant AMV change since AR6 has been the replacement of MTSAT-2 with Himawari-8. Himawari-8 has improved resolution and extra channels compared to MTSAT, and Himawari-8 AMVs are derived with new tracking and height assignment schemes. As a result of these changes the Himawari-8 AMVs have much smaller O-Bs than the MTSAT AMVs, shown for example in the updates on Features 2.8 and 2.9 (mid-level biases), 2.7 (fast low level winds) and 2.13 (high level fast bias in tropics). The improvements at low level come with the caveat that there now appear to be many AMVs assigned close to 1000 hPa. The satellite switchover also includes a large increase in data volume, which appears to provide better coverage of tropical cyclones (Feature 5.3).

There have also been significant changes to the EUMETSAT Metop products since AR6. The O-Bs were significantly improved following a derivation update in May 2014, particularly at mid level where the majority of polar AMV data is. However, as shown in Feature 7.2, a negative speed bias is now present at high level in the EUMETSAT Metop data - including in the new Dual-Metop AMVs. In the tropics, the Dual-Metop AMVs show an unexpected correlation between O-Bs and the zenith angle of the first image of the pair. This is believed to be because the height assignment is always done with the second image of the pair (Feature 7.1).

Other new data includes the stereo-height assigned MISR AMVs. These have reasonable O-Bs in general but in some cases there were issues with calibrating the cameras (Feature 7.5) and with tracking cloud shadows instead of the clouds themselves (Feature 7.3). Geostationary AMVs from INSAT-3D and COMS-1 have been added to the monitoring and in Features 2.8 and 2.9 it was seen that, at mid level, the COMS-1 AMVs have large differences to UKMO model backgrounds, while the INSAT-3D AMVs have small O-Bs but a low data volume. The FY-2 AMV derivation has undergone a series of changes which have decreased O-Bs in some cases and increased them in others (Features 2.8 and 2.13).

References

- [1] Shimoji, K., Motion tracking and cloud height assignment methods for Himawari-8 AMV, 2014, Proceeding from the 12 International Winds Workshop
- [2] FY-2 Algorithm Improvements (updated version of 'Status of Operational AMVs from FY-2 Satellites since the 11th Winds Workshop', Xiaohu Zhang, Jianmin Xu, Qisong Zhang, 2014.), courtesy of Jianmin Xu, 2016,
- [3] García-Pereda, J., Borde, R., The Impact of the Tracer Size and the Temporal Gap between Images in the Extraction of Atmospheric Motion Vectors, 2014, Journal of Atmospheric and Oceanic Technology, Volume 31, 1761-1770
- [4] AR5 (2012), Cotton, J., Fifth analysis of the data displayed on the NWP SAF AMV monitoring website, Document NWPSAF-MO-TR-027
- [5] AR6 (2014), Cotton, J., NWP SAF AMV monitoring: the 6th Analysis Report, Document NWPSAF-MO-TR-029

Acknowledgements

ECMWF statistics are routinely provided thanks to Mohamed Dahoui.

Thanks to Xu Jianmin (CMA), Kevin Mueller and Michael Garay (NASA-JPL), Jeff Key and David Santek (CIMSS), and Olivier Hauteceur (EUMETSAT) for helpful explanations.